RESEARCH ARTICLE
doi: 10.2306/scienceasia1513-1874.2021.S014

*ScienceAsia* 47S (2021): **69–75**

# Enhanced visible light response of $TiO_2$ nanoparticles by natural dyes

**Voranuch Somsongkul[a,b,*], Prae Chirawatkul[c], Chanapa Kongmark[d,*]**

[a] Department of Industrial Chemistry, Faculty of Applied Science, King Mongkut's University of Technology North Bangkok, Bangkok 10800 Thailand
[b] Integrated Chemistry Research Center for Sustainable Technology (ICRT), King Mongkut's University of Technology North Bangkok, Bangkok 10800 Thailand
[c] Synchrotron Light Research Institute (Public Organization), Suranaree University of Technology, Nakhon Ratchasima 30000 Thailand
[d] Specialized center of Rubber and Polymer Materials in agriculture and industry (RPM), Department of Materials Science, Faculty of Science, Kasetsart University, Bangkok 10900 Thailand

*Corresponding authors, e-mail: voranuch.s@sci.kmutnb.ac.th, chanapa.k@ku.th

*Received 11 Nov 2020*
*Accepted 10 Jun 2021*

**ABSTRACT**: The visible light responding $TiO_2$ nanoparticles have been achieved through green synthesis method. In this experiment, three types of natural dyes including Turmeric extract, Bergamot fruit extract, and Siamese neem leave extract were used as stabilizing agents. $TiO_2$ nanoparticles were synthesized by solution-based one-step and two-step methods. The results of X-ray diffraction (XRD) and Ti K-edge X-ray absorption near edge structure (XANES) spectroscopy affirmed that anatase $TiO_2$ nanoparticles were obtained from all samples with the average crystallite sizes of 5–8 nm. Moreover, UV-Visible absorption spectra revealed that the natural dyes play an important role in improving the visible light absorption ability of $TiO_2$ and decreasing the band gap energy of $TiO_2$ from 3.1 eV to 2.3 eV. The absorption edge energies of the two-step samples were lower than those of the one-step samples. The infrared spectra of the two-step $TiO_2$ displayed complex vibration features which were related to the carbonyl (C=O) and hydroxyl (O—H) groups of natural dyes. The presence of these functional groups was obviously responsible for the optical response of $TiO_2$ nanoparticles in the visible wavelength region.

**KEYWORDS**: $TiO_2$, natural dye, turmeric extract, bergamot fruit extract, Siamese neem leave extract

## INTRODUCTION

With the rapid worldwide growth in renewable energy, the development in energy conversion and storage systems are becoming increasingly important. $TiO_2$ is one of the most important semiconductors, and it is a potential candidate for use in photoelectrochemical (PEC) solar cells, supercapacitors, and Li-ion batteries. Fujishima and Honda first pointed out the application of water photoelectrochemical concept that employed the semiconductor properties of $TiO_2$ [1]. Its band gap energy is suitable for absorbing ultraviolet (UV) light, promoting electrons from the valence to the conduction band. In the PEC cell, composed of $TiO_2$ as *n*-type semiconductor photoelectrode, electrons and holes are generated when the $TiO_2$ is irradiated with UV light. The photogenerated electrons reduce water to form $H_2$ on Pt counter electrode, while holes oxidize water to form $O_2$ on the $TiO_2$ electrode with some external biases by a power supply or pH. However, the light absorption efficiency is rather moderate for commercial applications. The limitation of the $TiO_2$ for use as a photoelectrode is its poor visible light absorption due to wide band gap energy (ca. 3.0 eV for rutile and 3.2 eV for anatase) and high recombination rate of photogenerated electron-hole pairs. Several techniques for improving the photocatalytic activity of $TiO_2$ in visible light have been proposed [2], including doping technique with many types of dopants (metal ions and non-metal ions) [3] and reactive complex formation [4]. In the 1990s, Grätzel and co-workers proposed dye-sensitized solar cells technology by the successful combination of $TiO_2$ electrodes and synthetic organic dyes, resulting in greater efficiency of up to 7% [5]. The major challenge is not only to develop the visible light responding $TiO_2$ nanoparticles, but also the facile, nontoxic, and alternative low-cost synthesis method that can be widely used in many applications.

The green synthesis of metal nanoparticles has attracted much attention recently, for example, the green synthesis of silver nanoparticles using plant extract for heavy metal sensing [6]. For $TiO_2$ nanoparticles, various natural resources have been used for their biogenic syntheses [7,8]. $TiO_2$ nanoparticles were synthesized from titanium chloride using orange peel extract. The average crystallite size of the sample deduced from X-ray diffraction and the particle size deduced from particle size analyzer were 17 nm and 22 nm, respectively [9]. Besides, the $TiO_2$ particles obtained from titanium chloride using aloe vera extract had the particle size of 20–50 nm [10]. It has been reported that $TiO_2$ nanoparticles could be produced from titanium hydroxide using *Euphorbia heteradena Jaub* root extract as a reducing and stabilizing agent without application of toxic reagents or surfactant templates [11]. The *Echinacea purpurea* herba extract was also used as a bioreductant for the production of 120 nm $TiO_2$ nanoparticles [12]. However, most reports focused on the morphology and particle size of titania, while the structure and photo-physical properties under visible light region of titania have not been investigated. Alternative natural dyes abundant in Thailand, such as turmeric extract, bergamot fruit extract, and Siamese neem leave extract have been used as stabilizing agents to prevent agglomeration and achieve the desired shape and size of $TiO_2$ nanoparticles [13]. They are non-toxic and applicable without complicated purification. Moreover, the intense colors of these natural dyes would suggest that they have excellent visible light absorption abilities. Therefore, we can expect that the application of these natural dyes would shift the photocatalytic response of $TiO_2$ nanoparticles to the visible light region and prevent the electron-hole recombination. In addition, the existence of highly reactive (OH) groups in the dye structure can facilitate its attachment to titania surface.

In this study, three natural dyes (i.e., turmeric extract, bergamot fruit extract, and Siamese neem leave extract) have been used to synthesize $TiO_2$ nanoparticles by solution-based one-step ($TiO_2$-natural dye) and two-step ($TiO_2$/natural dye) methods. A facile synthesis method has been developed to produce the dye-functionalized titania nanoparticles and to extend the light absorption of $TiO_2$ into the visible region of the spectrum and. Therefore, improve its photocatalytic performance.

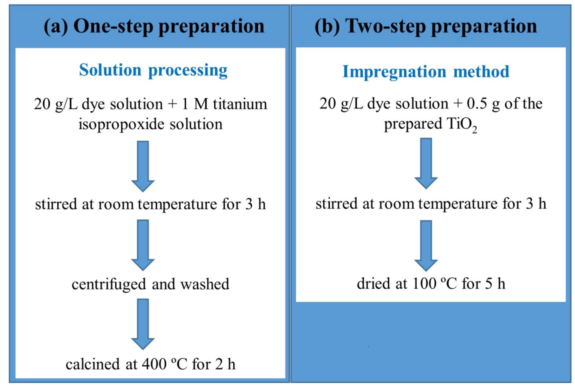


**Fig. 1** Natural dye assisted synthesis of $TiO_2$ nanoparticles by: (a) one-step method and (b) two-step method.

## MATERIALS AND METHODS

### Preparation of natural dyes

Aqueous extracts of turmeric, bergamot and Siamese neem were prepared from their respective components: fresh roots, peels, and leaves. Individual components were cleaned, and boiled with distilled water at 60 °C for 1 h. Then, the extracts were filtered through Whatman No. 1 filter papers and evaporated to obtain concentrated dyes.

### Synthesis of $TiO_2$ nanoparticles

$TiO_2$ nanoparticles were synthesized via sol-gel method using titanium isopropoxide solution as a starting material. The sample was prepared by dissolving 1 M titanium isopropoxide in 100 ml distilled water. The solution was subjected to constant stirring for 3 h at room temperature. (The formation of nanoparticles occurred during this process.) Then, the mixture was centrifuged at 3000 rpm for 15 min to separate the nanoparticles, which were later washed with distilled water repeatedly to remove the by-products. Finally, the nanoparticles were calcined at 400 °C for 2 h.

### Natural dye assisted synthesis of $TiO_2$ nanoparticles

Natural dye assisted $TiO_2$ nanoparticles were synthesized by solution-based one-step ($TiO_2$-natural dye) and two-step ($TiO_2$/natural dye) methods as shown in Fig. 1.

For the one-step preparation, 20 g/l dye solutions were individually added to 1 M titanium isopropoxide solutions under stirring at room temperature for 3 h. The mixtures were centrifuged, washed, and calcined at 400 °C for 2 h to obtain the

$TiO_2$-Turmeric, the $TiO_2$-Bergamot, and the $TiO_2$-Siamese neem nanoparticles.

For the two-step preparation, $TiO_2$/natural dye nanoparticles were prepared by wet impregnation method. 20 g/l dye solutions were individually added to 0.5 g of the prepared $TiO_2$. The solutions were subjected to constant stirring at room temperature for 3 h. The mixtures were dried at 100 °C for 5 h to obtain the $TiO_2$/Turmeric, the $TiO_2$/Bergamot, and the $TiO_2$/Siamese neem nanoparticles.

### Characterization of $TiO_2$ nanoparticles

The X-ray diffraction patterns were recorded by Bruker D8 advance diffractometer equipped with a Lynxeye position sensitive detector and Ni filter, in the 20–80° range (step 0.02 s/step), using CuKα radiation (λ = 1.54 Å). The local structure around Ti atoms was investigated using X-ray absorption spectroscopy (XAS) at Beamline 1.1W: Multiple X-ray Techniques, at the Synchrotron Light Research Institute (SLRI), Thailand (electron energy of 1.2 GeV, multipole wiggler, beam current 80–150 mA). The X-ray beam was monochromatized by a Si(111) double-crystal monochromator. The obtained XAS data were processed using the Athena graphical interface of the IFEFFIT software package [14]. Surface morphology of synthesized $TiO_2$ was characterized using FEI, Quanta 450 scanning electron microscope. The UV-Visible spectra were collected in diffuse reflectance mode using an Analytikjena Specord 210 plus UV-Vis spectrometer (320–800 nm). The Fourier-transform infrared (FTIR) spectra were recorded over a spectral range of 400–4000 $cm^{-1}$ (4 $cm^{-1}$ resolution) from Bruker Vertex 70 FTIR spectrometer.

## RESULTS AND DISCUSSION

The phase composition and crystal structure of all synthesized $TiO_2$ powders, including $TiO_2$ and natural dye assisted $TiO_2$ prepared by the one-step ($TiO_2$-natural dye) and the two-step ($TiO_2$/natural dye) methods, were investigated by X-ray powder diffraction (XRD), and the results are shown in Fig. 2. All synthesized $TiO_2$ powders exhibited main diffraction peaks at 2θ of 25.4° (101), 37.9° (004), 48.0° (200), 54.2° (105), and 62.6° (204), which corresponded to anatase phase of $TiO_2$, a tetragonal crystal structure with space group I41/amd (JCPDS 21-1272) [15]. There were no characteristic peaks of impurities observed in the $TiO_2$ and $TiO_2$-natural dye powders. However, a small additional peak (at 30.9°) was noticed in $TiO_2$/natural dye, which

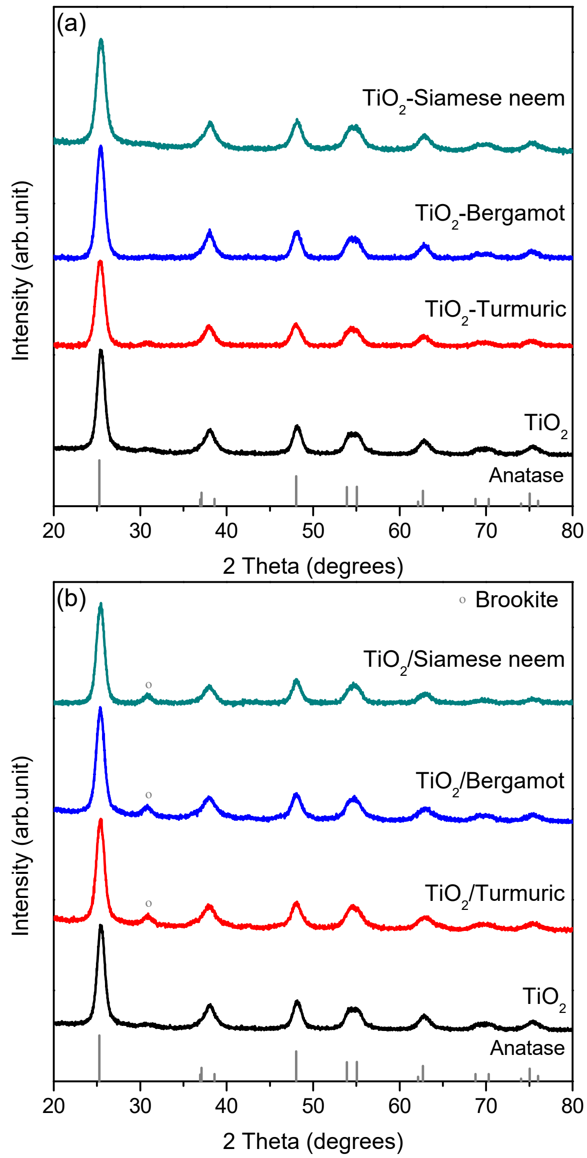


**Fig. 2** XRD patterns of $TiO_2$ nanoparticles compared with natural dye assisted $TiO_2$ nanoparticles prepared by: (a) one-step method and (b) two-step method.

was obviously due to the slight presence of brookite $TiO_2$ phase. The average crystallite size of $TiO_2$ nanoparticles was calculated from the diffraction peak width using Debye-Scherrer's formula:

$$D = \frac{K\lambda}{\beta \cos\theta}$$

where $D$ is the crystallite size, $\lambda$ is the wavelength of the X-ray radiation (0.15406 nm) for CuKα, $K$ is usually taken as 0.89, and $\beta$ is the full width at half maximum (FWHM) of the most intense diffraction

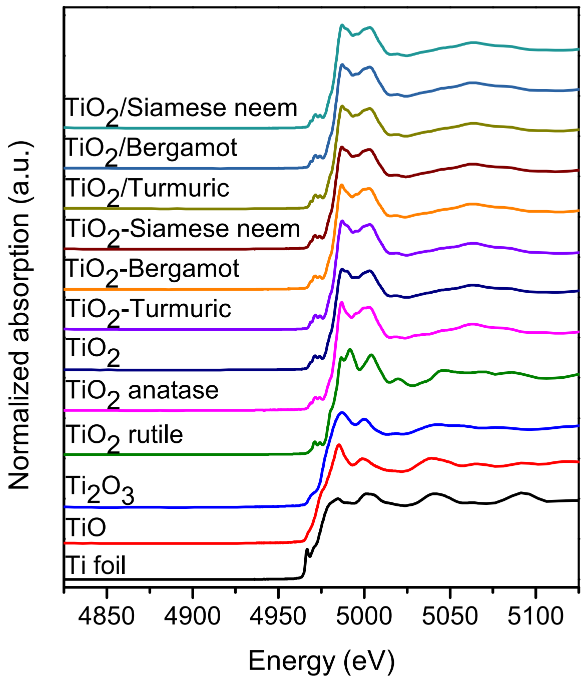


**Fig. 3** Ti K-edge XANES spectra of Ti references, $TiO_2$, nanoparticles, and natural dye assisted $TiO_2$ nanoparticles.

**Table 1** Average crystallite sizes of $TiO_2$ and natural dye assisted $TiO_2$ with one-step method ($TiO_2$-natural dye) and two-step method ($TiO_2$/natural dye) nanoparticles.

| Sample | The average crystallite sizes (nm) |
|---|---|
| $TiO_2$ | 7.07 |
| $TiO_2$-Turmeric | 6.82 |
| $TiO_2$-Bergamot | 7.12 |
| $TiO_2$-Siamese neem | 6.01 |
| $TiO_2$/Turmeric | 5.47 |
| $TiO_2$/Bergamot | 5.78 |
| $TiO_2$/Siamese neem | 7.56 |

peak (2θ at 25.493°). The obtained crystallite sizes are summarized in Table 1. The average crystallite sizes of all $TiO_2$ samples were in the range of 5–7 nm.

X-ray absorption spectroscopy (XAS) analyses provided additional information on the oxidation state and local atomic structure around Ti atoms in the synthesized $TiO_2$ particles. Ti K-edges X-ray absorption near edge structure (XANES) spectra of all $TiO_2$ samples and the reference compounds, i.e., Ti metal, TiO, $Ti_2O_3$, anatase, and rutile $TiO_2$, are presented in Fig. 3. At first glance, XANES spectrum of each reference material exhibited specific features because the edge energy position, pre-edge peak, and oscillation shape were specifically sensitive to the oxidation states and the local structure around the central atoms (Ti atoms). XANES spectra of all $TiO_2$ samples were identical to that of anatase $TiO_2$ standard. No evidence of the characteristic pre-edge and oscillation features from other titanium oxides were observed in XAS spectra of the $TiO_2$ and the natural assisted $TiO_2$ samples. These results affirmed the formation of anatase $TiO_2$ (dominated by $Ti^{4+}$ ions) as a main titanium compounds in all the samples.

The functional groups on the surface of $TiO_2$ and natural dye assisted $TiO_2$ nanoparticles were analyzed by Fourier-transform infrared spectroscopy (FTIR), and the results are illustrated in Fig. 4. All $TiO_2$ samples showed broad absorption bands between 400 $cm^{-1}$ and 800 $cm^{-1}$, mainly ascribed to Ti—O and Ti—O—Ti stretching modes, which affirmed the formation of $TiO_2$ particles [16, 17]. The absorption peaks between 3000 $cm^{-1}$ and 3800 $cm^{-1}$ were assigned to O—H stretching vibration mode of hydroxyl functional group. The absorption peaks at 1618 $cm^{-1}$ were characteristics of H—OH groups of $TiO_2$ [11]. The vibration bands at 1719 $cm^{-1}$ and 2960 $cm^{-1}$ in natural dye assisted $TiO_2$ by two-step preparations showed characteristics of C=O and C—H stretching absorptions, respectively [18]. This would suggest the presence of hydroxyl and carbonyl groups of the natural dyes on the $TiO_2$ surface, which would contribute to the photocatalytic activity of $TiO_2$ [19].

Fig. 5 shows the Scanning Electron Microscope (SEM) images revealing the surface morphology of $TiO_2$ and the natural dye assisted $TiO_2$ nanoparticles. All synthesized $TiO_2$ particles formed spherical agglomerates. The $TiO_2$-natural dye showed the smallest particle sizes (∼100–300 nm) compared with those obtained by the $TiO_2$/natural dye (∼500 nm) and those of $TiO_2$ (∼500 nm). The natural dye type had no significant influence on the particle size. It seems likely that the natural dye assisted synthesis with one-step method enhanced the dispersion of $TiO_2$ nanoparticles. This should be due to the steric hindrance effect of long-chain dye molecules that limits direct contact between particles, and therefore prevented particle agglomeration. A similar observation was previously reported by Bagwe et al [20]. The severe aggregation of silica nanoparticles could be reduced by adding functional groups, such as amine/phosphonate and

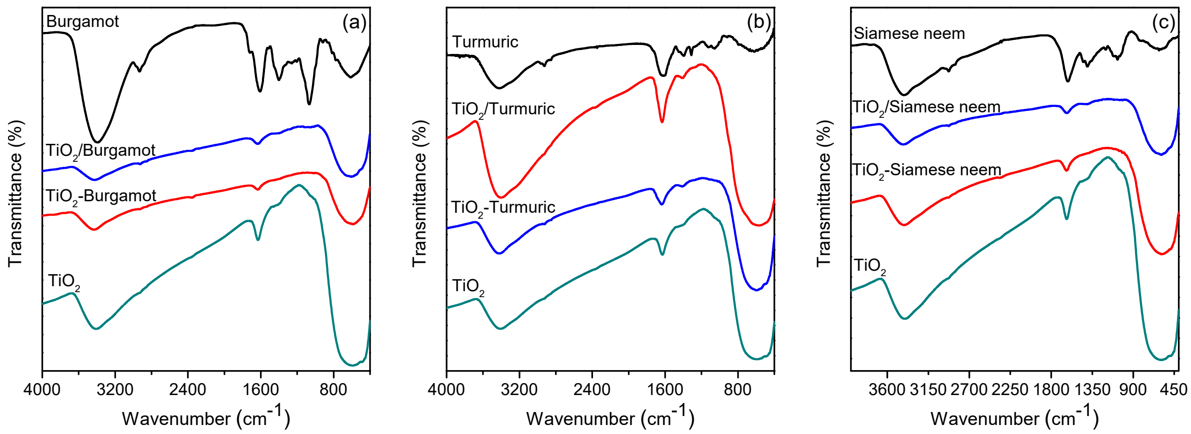


**Fig. 4** FTIR spectra of three series of natural dyes extracted from: (a) Burgamot fruit peels, (b) Turmuric roots, and (c) Siamese neem leaves.

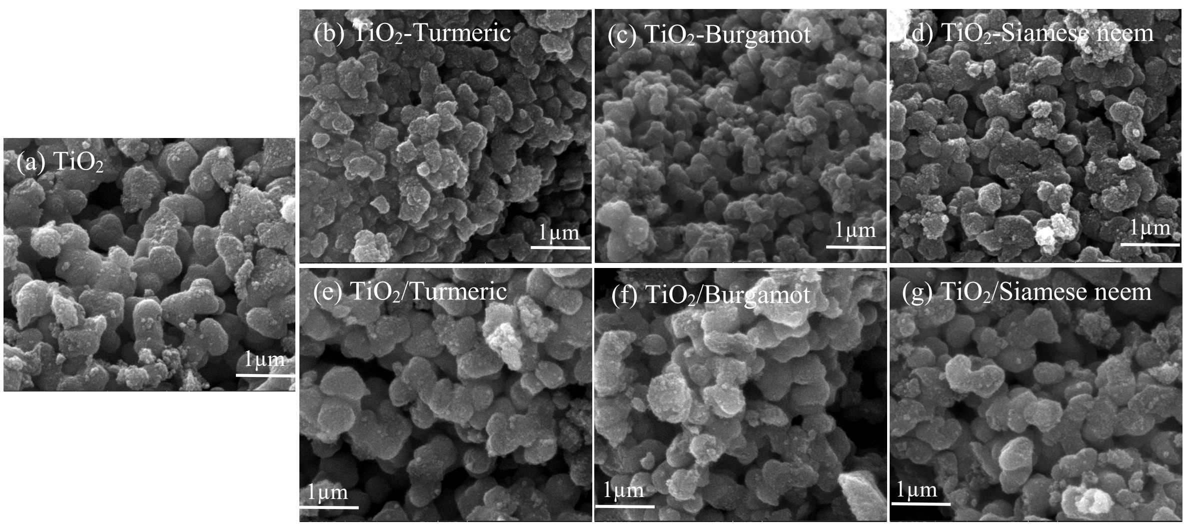


**Fig. 5** SEM images of (a) $TiO_2$, (b–d) one-step natural dye assisted $TiO_2$, and (e–g) two-step natural dye assisted $TiO_2$ nanoparticles.

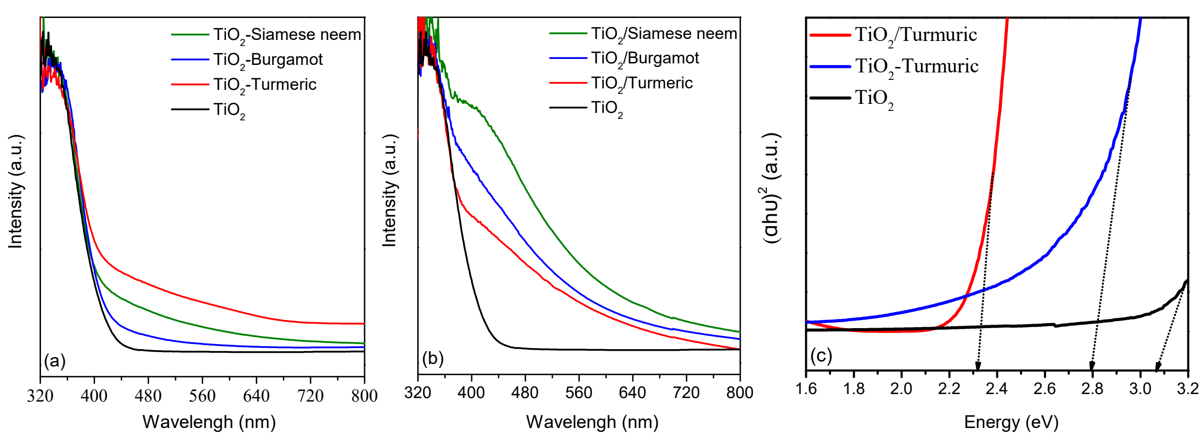


**Fig. 6** Absorption spectra of natural dye assisted $TiO_2$ nanoparticles prepared by: (a) one-step and (b) two-step methods; (c) plot of $(\alpha h\nu)^2$ versus photon energy ($h\nu$) for $TiO_2$, $TiO_2$-Turmeric and $TiO_2$/Turmeric nanoparticles.

carboxylate/octadecyl to the surface. The mechanism of electrostatic repulsion or steric hindrance-based stabilization for the prevention of surface-modified silica nanoparticle agglomeration was also demonstrated.

In this work, turmeric roots extract, bergamot fruit peels extract and neem leaves extract were used as photo-sensitizer to improve the visible light response of $TiO_2$. The optical properties of the synthesized $TiO_2$ nanoparticles were studied by means UV-Vis spectroscopy, as illustrated in Fig. 6. The $TiO_2$ prepared without natural dye exhibited a strong absorption in the 320–450 nm wavelength range. It is worth noting that the absorption of the natural dye assisted $TiO_2$ extended into the visible region of the spectrum, to wavelengths greater than 600 nm (Fig. 6ab). The one-step prepared $TiO_2$ ($TiO_2$-natural dye) had only a strong absorption peak (at about 320 nm) similar to that of $TiO_2$ while the two-step prepared $TiO_2$ ($TiO_2$/natural dye) also had a shoulder at longer wavelength (about 420 nm). In addition, the band gap energies of all $TiO_2$ samples were determined by applying Tauc's relation [21]. The optical absorbance coefficient of a semiconductor close to the band edge can be expressed by the following equation:

$$\alpha = \frac{A(h\nu - E_g)^n}{h\nu}$$

where $\alpha$ïĂă is the absorption coefficient, $A$ is the absorption constant, $h$ is the Planck's constant (J.s), $E_g$ is the band gap energy, $n = 1/2$ for direct allowed transition [22]. An example of the plot of $(\alpha h\nu)^2$ versus photon energy ($h\nu$) is presented in Fig. 6c. The extrapolation of the plot to the intercept yielded the direct band gap energy, $E_g$, for these materials. The band gap energy values of $TiO_2$ and natural dye assisted $TiO_2$ were summarized in Table 2. In general, the natural dye assisted $TiO_2$ prepared by the two-step method showed the lowest band gap energies (2.31–2.41 eV) compared to those obtained by the one-step method (2.79–3.13 eV) and those of $TiO_2$ (3.07 eV). The band gap energy values of the two step prepared $TiO_2$ were: $TiO_2$/Turmeric (2.31 eV) < $TiO_2$/Siamese neem (2.34 eV) < $TiO_2$/Bergamot (2.41 eV). These band gap values correlated well with the energy absorption results that the natural dye assisted $TiO_2$ prepared by the two-step method had the small band gap values, consequently had the great visible light absorption ability.

**Table 2** Band gap energies of $TiO_2$ and natural dye assisted $TiO_2$ with one-step method ($TiO_2$-natural dye) and two-step method ($TiO_2$/natural dye) nanoparticles.

| Sample | Band gap energy (eV) |
|---|---|
| $TiO_2$ | 3.07 |
| $TiO_2$-Turmeric | 2.79 |
| $TiO_2$-Bergamot | 3.13 |
| $TiO_2$-Siamese neem | 3.04 |
| $TiO_2$/Turmeric | 2.31 |
| $TiO_2$/Bergamot | 2.41 |
| $TiO_2$/Siamese neem | 2.34 |

## CONCLUSION

The natural dye assisted $TiO_2$ were successfully synthesized by solution-based one-step ($TiO_2$-natural dye) and two-step ($TiO_2$/natural dye) methods. XRD and XAS analyses affirmed the formation of anatase $TiO_2$ nanoparticles with the average crystallite sizes of 5–8 nm in all samples. It was found that the natural dye assisted synthesis with one-step method enhanced the dispersion of $TiO_2$ nanoparticles, resulting in particle size reduction, whereas the two-step synthesis method favored the deposition of natural dye molecules on the $TiO_2$ surface. UV-Vis spectroscopy study has demonstrated that the use of natural dye assisted synthesis method could extend the light absorption of $TiO_2$ into the visible range of the spectrum (wavelengths greater than 600 nm) and decrease the band gap energy of $TiO_2$ from 3.1 eV to 2.3 eV. The $TiO_2$ prepared by the two-step method provided lower absorption edge energies compared with those of the one-step. Their band gap energy values also varied depending on the dye type: $TiO_2$/Turmeric (2.31 eV) < $TiO_2$/Siamese neem (2.34 eV) < $TiO_2$/Bergamot (2.41 eV). Therefore, the natural dye assisted synthesis can be considered as a promising preparation method to improve the visible light absorption ability of metal oxide nanoparticles. We expected that this approach may offer a great advantage with respect to the preparation of nanocrystalline metal oxides, which are suitable for photocatalysis and photoelectrochemical applications.

*Acknowledgements*: The authors gratefully acknowledge the funding of the research from Thailand Research Fund, Office of the Higher Education Commission (Contract no. MRG6180084) and King Mongkut's University of Technology North Bangkok (Contract no. KMUTNB-ART-60-094). We also sincerely thank the Beamline 1.1W, Synchrotron Light Research Institute (Public Organization), Thailand for supporting XAS measurements.

## REFERENCES


1. Fujishima A, Honda K (1972) Electrochemical photolysis of water at a semiconductor electrode. *Nature* **238**, 37–38.
2. Bak T, Nowotny J, Rekas M, Sorrell CC (2002) Photoelectrochemical hydrogen generation from water using solar energy. Materials-related aspects. *Int J Hydrogen Energy* **27**, 991–1022.
3. Ward MD, Bard AJ (1982) Photocurrent enhancement via trapping of photogenerated electrons of $TiO_2$ particles. *J Phys Chem* **86**, 3599–3605.
4. Butler EC, Davis AP (1993) Photocatalytic oxidation in aqueous $TiO_2$ suspensions: the influence of dissolved transition metals. *J Photochem Photobiol A* **70**, 273–283.
5. Regan BO, Grätzel M (1991) A low-cost, high-efficiency solar cell based on dye-sensitized colloidal $TiO_2$ films. *Nature* **353**, 737–740.
6. Siraj M, Shah ZA, Ullah S, Bibi H, Suleman M, Zia A, Masood T, Iqbal Z, et al (2020) Biosynthesized silver nanoparticles from shoot and seed extracts of *Asphodelus tenufolius* for heavy metal sensing. *ScienceAsia* **46**, 697–705.
7. Mittal AK, Chisti Y, Banerjee UC (2013) Synthesis of metallic nanoparticles using plant extracts. *Biotechnol Adv* **31**, 346–356.
8. Irshad MA, Nawaz R, Rehman MZ, Adrees M, Rizwan M, Ali S, Ahmad S, Tasleem S (2021) Synthesis, characterization and advanced sustainable applications of titanium dioxide nanoparticles: A review. *Ecotoxicol Environ Saf* **212**, ID 111978.
9. Amanulla AM, Sundaram R (2019) Green synthesis of $TiO_2$ nanoparticles using orange peel extract for antibacterial, cytotoxicity and humidity sensor applications. *Mater Today Proc* **8**, 323–331.
10. Rajkumaria J, Magdalane CM, Siddhardha B, Madhavan J, Ramalingam G, Al-Dhabi NA, Arasu MV, Ghilan AKM, et al (2019) Synthesis of titanium oxide nanoparticles using *Aloe barbadensis mill* and evaluation of its antibiofilm potential against *Pseudomonas aeruginosa* PAO1. *J Photochem Photobiol B Biol* **201**, ID 111667.
11. Nasrollahzadeh M, Sajadi SM (2015) Synthesis and characterization of $TiO_2$ nanoparticles using *Euphorbia heteradena Jaub* root extract and evaluation of their stability. *Ceram Int* **41**, 14435–14439.
12. Dobrucka R (2017) Synthesis of $TiO_2$ nanoparticles using *Echinacea purpurea* herba. *Iran J Pharm Res* **16**, 753–759.
13. Sethy NK, Arif Z, Mishra PK, Kumar P (2020) Green synthesis of $TiO_2$ nanoparticles from *Syzygium cumini* extract for photo-catalytic removal of lead (Pb) in explosive industrial wastewater. *Green Process Synth* **9**, 171–181.
14. Ravel B, Newville M (2005) *ATHENA*, *ARTEMIS*, *HEPHAESTUS*: data analysis for X-ray absorption spectroscopy using *IFEFFIT*. *J Synchrotron Rad* **12**, 537–541.
15. Xu J, Li L, Yan Y, Wang H, Wang X, Fu X, Li G (2008) Synthesis and photoluminescence of well-dispersible anatase $TiO_2$ nanoparticles. *J Colloid Interface Sci* **318**, 29–34.
16. Zhao Y, Li C, Liu X, Gu F, Jiang H, Shao W, Zhang L, He Y (2007) Synthesis and optical properties of $TiO_2$ nanoparticles. *Mater Lett* **61**, 79–83.
17. Ruhane TA, Islam MT, Rahaman MdS, Bhuiyan MMH, Islam JMM, Bhuiyan TI, Khan K, Khan MA (2017) Impact of photo electrode thickness and annealing temperature on natural dye sensitized solar cell. *Sustain Energy Technol Assess* **20**, 72–77.
18. Maiaugree W, Lowpa S, Towannang M, Rutphonsan P, Tangtrakarn A, Pimanpang S, Maiaugree P, Ratchapolthavisin N, et al (2015) A dye sensitized solar cell using natural counter electrode and natural dye derived from mangosteen peel waste. *Sci Rep* **5**, ID 15230.
19. Narayan MR (2012) Review: Dye sensitized solar cells based on natural photosensitizers. *Renew Sustain Energy Rev* **16**, 208–215.
20. Bagwe RP, Hilliard LR, Tan W (2006) Surface modification of silica nanoparticles to reduce aggregation and nonspecific binding. *Langmuir* **22**, 4357–4362.
21. Tauc J, Grigorovici R, Vancu A (1966) Optical properties and electronic structure of amorphous germanium. *Phys Status Solidi B* **15**, 627–637.
22. Mandal S, Jain N, Pandey MK, Sreejakumari SS, Shukla P, Chanda A, Som S, Das S, et al (2019) Ultrabright emission from Sr doped $TiO_2$ nanoparticles through r-GO conjugation. *R Soc Open Sci* **6**, ID 190100.